PHYSICAL REVIEW A **85**, 061602(R) (2012)

Universal probes for antiferromagnetic correlations and entropy in cold fermions on optical lattices

E. V. Gorelik,[1] D. Rost,[1] T. Paiva,[2] R. Scalettar,[3] A. Klümper,[4] and N. Blümer[1]
[1]*Institute of Physics, Johannes Gutenberg University, Mainz, Germany*
[2]*Instituto de Fisica, Universidade Federal do Rio de Janeiro, Rio de Janeiro, Brazil*
[3]*Department of Physics, University of California, Davis, California 95616, USA*
[4]*University of Wuppertal, Wuppertal, Germany*
(Received 18 May 2011; revised manuscript received 20 March 2012; published 7 June 2012)

We determine antiferromagnetic (AF) signatures in the half-filled Hubbard model at strong coupling on a cubic lattice and in lower dimensions. Upon cooling, the transition from the charge-excitation regime to the AF Heisenberg regime is signaled by a universal minimum of the double occupancy at entropy $s \equiv S/(Nk_{\mathrm{B}}) = s^* \approx \ln(2)$ per particle and a linear increase of the next-nearest-neighbor (NNN) spin correlation function for $s < s^*$. This crossover, driven by a gain in kinetic exchange energy, appears as the essential AF physics relevant for current cold-atom experiments. The onset of long-range AF order (at low s on cubic lattices) is hardly visible in nearest-neighbor spin correlations versus s, but could be detected in spin correlations at or beyond NNN distances.

DOI: 10.1103/PhysRevA.85.061602 PACS number(s): 67.85.−d, 03.75.Ss, 71.10.Fd, 75.10.−b

Materials with strong electronic correlations are, due to their increasing technological importance, a prime subject of current research [1,2]. Theoretical investigations of corresponding Hubbard-type models have shed light on many strong-coupling phenomena, including metal-insulator transitions, non-Fermi-liquid behavior, and various types of magnetic and orbital order [3]. However, important questions remain open, most notably regarding high-temperature superconductivity, for which a mechanism is needed. Recently, a novel class of correlated Fermi systems, namely, ultracold fermionic atoms (such as ^{40}K and ^{6}Li) on optical lattices, has opened a new promising direction of research: Cold atoms are predicted to serve as *quantum simulators* for the Hubbard-type solid-state Hamiltonians of interest [4–6].

Indeed, the Mott metal-insulator transition has recently been demonstrated in two-flavor mixtures of ^{40}K on cubic optical lattices by experimental observation and quantitative theoretical analysis of signatures in the compressibility [7] and in the double occupancy [8]. This success established that the single-band Hubbard model

$$\hat{H} = -t \sum_{\langle ij\rangle,\sigma} \hat{c}^{\dagger}_{i\sigma}\hat{c}_{j\sigma} + U \sum_{i} \hat{n}_{i\uparrow}\hat{n}_{i\downarrow} \qquad (1)$$

(with hopping amplitude t, on-site interaction U, and $\hat{n}_{i\sigma} = \hat{c}^{\dagger}_{i\sigma}\hat{c}_{i\sigma}$) can be realized to a reasonable accuracy using ultracold fermions in the interesting interaction range, which certainly supports the hopes of accessing also less understood Hubbard physics in similar ways.

However, attempts to realize and detect *quantum magnetism* in cold lattice fermions have proven extremely challenging. In fact, it is even difficult to verify specific signatures of antiferromagnetic (AF) correlations which are believed to play an important role in high-temperature superconductivity. This type of physics clearly has to be under control before cold fermions on optical lattices can really play a useful role as *quantum simulators* of materials with strong electronic correlations. The failure to detect AF signals has primarily been attributed to cooling issues [9,10]. Indeed, the coldest experiments for repulsive fermions on optical lattices have thus far reached central entropies per particle of $s \equiv S/(Nk_B) \approx \ln(2) \approx 0.7$ [11,12] while AF long-range order (LRO) on an isotropic cubic lattice is expected only for entropies $s < s_{\mathrm{N}} \approx 0.4$ [9,13,14].

An important feature of cold-atom systems is their inhomogeneity, induced by the trapping potential. On the one hand, this is beneficial for quantum magnetism, since entropy is effectively pushed out of a half-filled core; this aspect is a major theme of current research [11,14–17]. On the other hand, any AF region will necessarily be of limited spatial extent [18], so that the thermodynamic concept of LRO is not fully applicable. In addition, as we will show, the nearest-neighbor (NN) spin correlation function, which is currently addressed (using modulation spectroscopy [9,19] or superlattices [20]) in AF-related experiments, is hardly sensitive to the onset of LRO even in the thermodynamic limit.

In this situation, one may ask the following: (i) Is there a threshold distance beyond which spin correlations have "long-range characteristics" and (ii) can we define "finite-range antiferromagnetism" as a unique scenario with universal properties, appearing only in a certain entropy range? The answer to both questions is "yes": The essential AF correlation physics emerges already at entropies $s \lesssim \ln(2)$, i.e., in reach of current cooling techniques. Since, in addition, the threshold distance turns out to be rather small (but larger than one lattice spacing), our quantitative predictions should enable experimentalists to verify specific AF signatures with current system sizes, i.e., to get the long-sought grip on *quantum magnetism*.

In the following, we discuss first an enhancement of the double occupancy D (i.e., also of the interaction energy $E_{\mathrm{int}} \equiv D\,U$) at low temperatures T which has previously been proposed as an AF signature on the basis of dynamical mean-field theory (DMFT) [21]. DMFT results for a half-filled cubic lattice at strong coupling $U/t = 15$ are compared with direct determinantal quantum Monte Carlo (DQMC) [22,23] simulations. The comparison is extended to the full dimensional range based on DQMC and Bethe ansatz (BA) [24] data in dimensions $d = 2$ and $d = 1$, respectively. High-precision estimates of the entropy $s(T)$ allow us to switch to the experimentally relevant entropy representation. An

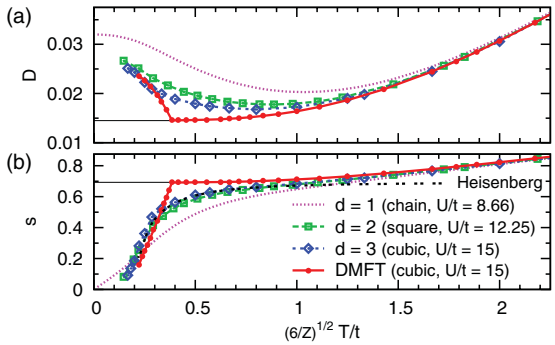

FIG. 1. (Color online) Hypercubic lattice ($1 \leqslant d \leqslant 3$) at strong coupling $U/(\sqrt{Z}t) \approx 6$: (a) Double occupancy $D(T)$ as estimated from DMFT ($d = 3$, circles), DQMC ($d = 3$: diamonds; $d = 2$: squares), and BA ($d = 1$, dotted line). (b) Corresponding estimates of entropy per particle $s = S/(Nk_B)$.

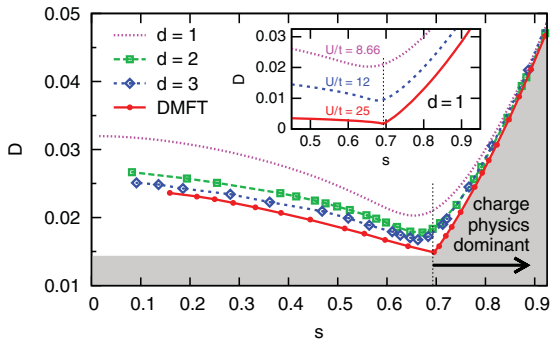

FIG. 2. (Color online) Hypercubic lattice at strong coupling: Double occupancy vs entropy. In all cases, the minimum of the double occupancy corresponds to $s^* \approx \ln(2)$ (dotted line). The shaded area indicates the nonmagnetic contribution to D. Inset: $D(s)$ in $d = 1$ for various interactions.

asymptotic collapse of the curves $D(s)$ is observed with respect to dimensionality, with universal minima at $s^* \approx \ln(2)$, and no significant features at s_N in the cubic case. Additional specific signatures of finite-range AF order are found in the kinetic energy and in spin correlation functions, with different degrees of universality. Finally, the perspectives for detecting LRO are discussed using stochastic series expansion (SSE) results for the Heisenberg model.

AF signatures in the double occupancy. According to DMFT, the low-T formation of an AF core in a fermionic cloud on an optical lattice (with central half filling, $n = 1$) is signaled, at strong coupling, by a distinct enhancement of D in the same region [21]. As a function of temperature, DMFT predicts nearly flat curves $D(T)$ in the range $T \gtrsim T_N^{\mathrm{DMFT}}$, i.e., above its estimate of the Néel temperature, and a sharp increase below, with a kink and absolute minimum at T_N^{DMFT}. This is clearly seen, for $U/t = 15$, in Fig. 1(a) (circles). The absolute low-T increase of D is largest for $U/t \approx 12$; it should be detectable, according to real-space DMFT, even in experiments integrating over the inhomogeneous cloud [21].

Not all aspects of this DMFT scenario are, however, realistic: After all, DMFT is exact only in the limit of infinite coordination number $Z \to \infty$ (with $Z = 2d$ for hypercubic lattices) and overestimates the Néel temperature by up to 30% in the simple cubic case [25,26]. Thus, the sharp kink in $D(T)$ seen in Fig. 1(a) at $T_N^{\mathrm{DMFT}} \approx 0.4t$ cannot be physical. One might expect a shift of the DMFT results toward *lower* temperatures, as well as some broadening in the cubic case and more radical changes (at least) for $d \leqslant 2$; only at high temperatures does the accuracy of DMFT estimates for D follow already from series expansions (in $d = 3$) [27].

Impact of dimensionality. Indeed, DQMC estimates of $D(T)$ [diamonds in Fig. 1(a)] agree with DMFT for $T/t \gtrsim 1$ within error bars, which are smaller than symbol sizes [28]. Surprisingly good agreement is observed also at $T/t \lesssim 0.3$. As expected [21], the DMFT kink is smeared out in the DQMC data toward a broad minimum. At suitably rescaled [32] interactions, DQMC data for $d = 2$ (squares) show remarkably similar behavior. Only the case $d = 1$ (dotted line) deviates more drastically at intermediate and low T. Note that the position of the minimum in $D(T)$ shifts *upward* with decreasing d, i.e., opposite to the naive expectation.

As optical lattice and interactions are switched on for the ultracold atoms in a nearly adiabatic process [11], the entropy s (and not T) is the experimentally relevant control parameter. Figure 1(b) shows numerically exact data for $s(T)$, obtained directly for $d = 1$ and via the thermodynamic relation $S(\beta) = \ln(4) + \beta E(\beta) - \int_0^\beta d\beta' E(\beta')$ [with $\beta = 1/(k_B T)$ and energy E] for $d = 2,3$ and DMFT. Again, the agreement between $d = 2$ and $d = 3$ is striking; the latter results converge to the Heisenberg limit for $T \lesssim 0.8t$. Remarkably, the proper DMFT solution (circles) is close to the DQMC result for the cubic lattice (diamonds) at $T \lesssim 0.3t$; only the metastable nonmagnetic DMFT solution (thin solid lines), considered in previous studies [27], remains far off.

Figure 2, obtained by combining the data of both panels of Fig. 1, conveys our first central message: As a function of entropy, the double occupancy is surprisingly universal at strong coupling, with a minimum at $s^* \approx \ln(2)$ in all dimensions and generally similar shapes. At constant rescaled interaction U, the curvature around the minimum increases with increasing dimensionality until it becomes sharp in the DMFT limit, where it corresponds to the Néel transition. As seen in the inset (for $d = 1$), the minimum becomes also sharp and approaches s^* at constant dimensionality in the strong-coupling limit $U \to \infty$. Evidently, the minimum in $D(s)$ separates two regimes with quite different physical properties: (i) the regime $s > s^*$, which smoothly approaches the Hartree limit (with $D = \langle n_\uparrow \rangle \langle n_\downarrow \rangle = 0.25$) for $T \to \infty$, and (ii) a low-temperature regime, with no discernible substructure. It is clear that the latter regime must be characterized by spin coherence, since $s < \ln(2)$ can occur in a two-flavor system at $n = 1$ only by the development of (possibly short-ranged) magnetic correlations.

In fact, any positive deviation of $D(s)$ from the nonmagnetic background (shaded in Fig. 2) should be linked to AF correlations, generalizing Takahashi's ground-state expression [34]

$$D_0 = \frac{Zt^2}{2U^2}\left(1 - \langle \hat{\boldsymbol{\sigma}}_i \cdot \hat{\boldsymbol{\sigma}}_j \rangle_0^{\mathrm{Heis}}\right) + O\left(\frac{t^4}{U^4}\right). \qquad (2)$$

Here, $\langle \hat{\boldsymbol{\sigma}}_i \cdot \hat{\boldsymbol{\sigma}}_j \rangle_0^{\mathrm{Heis}}$ is the nearest-neighbor correlation in the quantum Heisenberg model at $T = 0$ (for Pauli matrices $\hat{\boldsymbol{\sigma}}$),

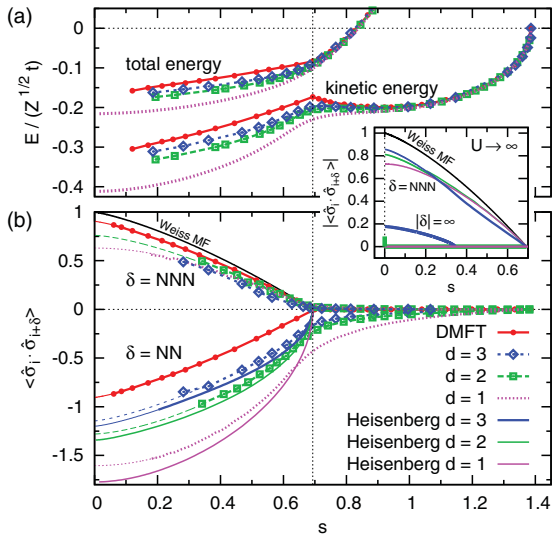

FIG. 3. (Color online) Hypercubic lattice at strong coupling: (a) Rescaled total and kinetic energy vs entropy. (b) Spin correlations $\langle \hat{\boldsymbol{\sigma}}_i \cdot \hat{\boldsymbol{\sigma}}_{i+\delta} \rangle$ between nearest [$\delta_{d=1} = 1$, $\delta_{d=2} = (1,0)$, $\delta_{d=3} = (1,0,0)$] and next-nearest [$\delta_{d=1} = 2$, $\delta_{d=2} = (1,1)$, $\delta_{d=3} = (1,1,0)$] neighbors. Inset: NNN and infinite-range correlations for Heisenberg model ($d = 1$ from Ref. [38]).

which is stronger in lower d:

$$\langle \hat{\boldsymbol{\sigma}}_i \cdot \hat{\boldsymbol{\sigma}}_j \rangle_0^{\mathrm{Heis}} = \begin{cases} -1.77\,(d=1)\,[34], & -1.20\,(d=3)\,[36], \\ -1.34\,(d=2)\,[35], & -1.00\,(d=\infty), \end{cases}$$

consistent with our finite-T results. Thus, irrespective of the measurement technique, signatures of AF correlations may be easier to detect experimentally, at fixed s, for lower (effective) dimensionality. Conversely, a tuning of the hopping amplitude in z direction could help to discriminate magnetic effects from those of charge excitations; similar ideas involving frustration will be explored in a separate publication [37].

Energetics and spin correlations. Up to a numerical prefactor (of $15/\sqrt{6}$), the curves in Fig. 2 represent the rescaled interaction energy $E_{\mathrm{int}}/(\sqrt{Z}t)$. Complementary AF signatures appear in the kinetic energy, shown in Fig. 3(a). In particular, $E_{\mathrm{kin}}(s)$ exhibits a maximum at $s \approx s^*$ for $d \geqslant 3$ [while thermodynamic consistency ensures a monotonous total energy $E(s) = E_{\mathrm{int}}(s) + E_{\mathrm{kin}}(s)$]. The associated redistribution of quasimomentum at $s \lesssim s^*$ might be a worthwhile experimental target.

As mentioned in the introduction, nearest-neighbor (NN) spin correlations are, so far, playing a central role in the experimental quest for AF signatures in cold lattice fermions. However, as seen in the lower part of Fig. 3(b), the NN spin correlation functions (symbols and dashed and dotted lines) have strong high-entropy tails in all physical dimensions $d \leqslant 3$, with only trivial features at $s \approx s^*$, below which the Heisenberg model (solid lines) becomes applicable. Conclusions concerning the presence or proximity of AF order could be drawn from corresponding experimental data only via theoretical lookup tables.

In contrast, the next-nearest-neighbor (NNN) spin correlation functions are essentially zero for $s > s^*$ and take off linearly below in all dimensions. So the mere presence

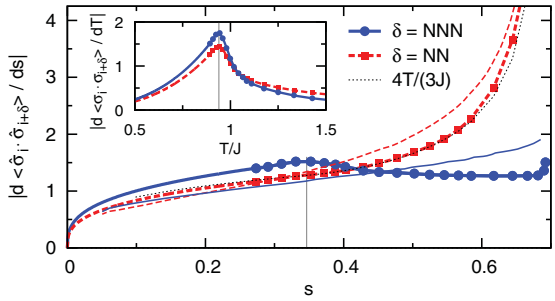

FIG. 4. (Color online) Derivatives of NN (squares) and NNN (circles) spin correlation functions of the Heisenberg model with respect to entropy (main panel) and temperature (inset) in $d = 3$. Thin solid and dashed lines: Heisenberg results in $d = 2$.

of significant NNN correlations already implies that the Heisenberg regime $s < \ln(2)$ has been reached. Remarkably, the results for $d = 1$ and $d = 2$ are indistinguishable (and close to DMFT) for $s \gtrsim 0.5$; only those for $d = 3$ are slightly below. The same picture emerges in the Heisenberg model (upper set of curves in the inset of Fig. 3), with slightly larger absolute values. This near universality with respect to d establishes that the crossing point between short-range physics, where spin correlations increase with lowering d, and long-range physics, where spin correlations decay quickly toward low d (and remain finite in the limit of distance $\delta \to \infty$ at $s > 0$ only for $d \geqslant 3$ [39], cf. the lower set of curves in the inset of Fig. 3) is essentially at the NNN distance.

In this sense, spin correlations at or beyond the NNN distance are much more representative of genuine AF physics than the unspecific NN correlations. This is true even regarding LRO, as illustrated in the Heisenberg limit (chosen due to the higher achievable accuracy) in Fig. 4:

While the entropy derivatives of the NN spin correlations in $d = 3$ (squares) are featureless [as those of the spin correlations in $d = 2$ (thin lines)], a distinct peak at the critical entropy s_{N} for AF LRO in $d = 3$ [13] is visible in the NNN data (circles), with a nearly flat plateau above. As a comparison with corresponding T derivatives (with clear peaks at T_N both in the NN and NNN data—see the inset of Fig. 4) shows, this qualitative difference is associated with the use of the entropy as a control parameter. With experiments being confined to this entropy parametrization [41], it is clear that a detection of the Néel transition via spin correlations would require measurements at least at NNN distances.

Conclusion. We have disentangled generic aspects of antiferromagnetism both from those specific to infinite-range order (which is not attainable, by definition, in finite atomic clouds) and from trivial nearest-neighbor correlations that persist even at high temperatures, where spin models are not adequate. Our results establish that the regime $s \lesssim s^* \approx \ln(2)$ is characterized by "finite-range antiferromagnetism" with remarkably universal properties. It may be detected experimentally, at strong coupling, by a negative slope in $D(s)$ [or $D(T)$] or by the onset of longer-range (beyond NN) spin correlations [42]. Long-range order appears inessential in the cold-atom context and largely decoupled from the basic correlation mechanisms (cf. recent iron layer experiments [43]): The mean-field critical entropy s^* is experimentally

more relevant than the critical entropy of an infinite system (in $d = 3$) [44]. Thus, reaching $s < s_N \approx 0.4$ in cubic systems would not guarantee additional insight and global equilibration (the time scales for which may exceed experimental life times [46]) is not essential. Tuning the dimensionality (and/or adding frustration) for discriminating AF effects appears much more promising.

Acknowledgments. We thank M. Inoue for help with the BA code, and P. G. J. van Dongen, U. Schneider, R. P. Singh, and L. Tarruell for valuable discussions. Support under ARO Award W911NF0710576 with funds from the DARPA OLE Program, by CNPq, FAPERJ, and INCT on Quantum Information, and by the DFG through SFB/TRR 49 and FOR 1346 is gratefully acknowledged.

[1] Y. Tokura, Phys. Today **56** (7), 50 (2003).
[2] E. Dagotto, Science **309**, 257 (2005).
[3] V. Anisimov and Y. Izyumov, *Electronic Structure of Strongly Correlated Materials*, Springer Series in Solid-State Sciences, Vol. 163 (Springer, Berlin, 2010).
[4] W. Hofstetter, J. I. Cirac, P. Zoller, and E. Demler, and M. D. Lukin, Phys. Rev. Lett. **89**, 220407 (2002).
[5] D. Jaksch and P. Zoller, Ann. Phys. (NY) **315**, 52 (2005).
[6] T. Esslinger, Annu. Rev. Condens. Matter Phys. **1**, 129 (2010).
[7] U. Schneider, L. Hackermuller, S. Will, Th. Best, I. Bloch, T. A. Costi, R. W. Helmes, D. Rasch, and A. Rosch, Science **322**, 1520 (2008).
[8] R. Jördens, N. Strohmaier, K. Günter, H. Moritz, and T. Esslinger, Nature (London) **455**, 204 (2008).
[9] D. Greif, L. Tarruell, T. Uehlinger, R. Jördens, and T. Esslinger, Phys. Rev. Lett. **106**, 145302 (2011).
[10] D. C. McKay and B. DeMarco, Rep. Prog. Phys. **74**, 054401 (2011).
[11] R. Jördens, L. Tarruell, D. Greif, T. Uehlinger, N. Strohmaier, H. Moritz, T. Esslinger, L. De Leo, C. Kollath, A. Georges, V. Scarola, L. Pollet, E. Burovski, E. Kozik, and M. Troyer, Phys. Rev. Lett. **104**, 180401 (2010).
[12] Note that the *average* entropy per particle in an trapped system is always larger, typically by a factor of about 2, than the entropy s per particle in the half-filled center.
[13] S. Wessel, Phys. Rev. B **81**, 052405 (2010).
[14] S. Fuchs, E. Gull, L. Pollet, E. Burovski, E. Kozik, Th. Pruschke, and M. Troyer, Phys. Rev. Lett. **106**, 030401 (2011).
[15] S. Chiesa, C. N. Varney, M. Rigol, and R. T. Scalettar, Phys. Rev. Lett. **106**, 035301 (2011).
[16] T. Paiva, Y. L. Loh, M. Randeria, R. T. Scalettar, and N. Trivedi, Phys. Rev. Lett. **107**, 086401 (2011).
[17] E. Khatami and M. Rigol, Phys. Rev. A **84**, 053611 (2011).
[18] Current experimental trap geometries ($\sim 10^5$ fermions) imply AF cores smaller than $40 \times 40 \times 20$ lattice sites, i.e., each AF site will "feel" a boundary within ten sites.
[19] C. Kollath, A. Iucci, I. P. McCulloch, and T. Giamarchi, Phys. Rev. A **74**, 041604(R) (2006).
[20] S. Trotzky, Y.-A. Chen, U. Schnorrberger, P. Cheinet, and I. Bloch, Phys. Rev. Lett. **105**, 265303 (2010).
[21] E. V. Gorelik, I. Titvinidze, W. Hofstetter, M. Snoek, and N. Blümer, Phys. Rev. Lett. **105**, 065301 (2010); N. Blümer and E. V. Gorelik, Comput. Phys. Commun. **118**, 115 (2011).
[22] R. Blankenbecler, D. J. Scalapino, and R. L. Sugar, Phys. Rev. D **24**, 2278 (1981).
[23] T. Paiva, R. Scalettar, M. Randeria, and N. Trivedi, Phys. Rev. Lett. **104**, 066406 (2010).
[24] G. Jüttner, A. Klümper, and J. Suzuki, Nucl. Phys. B **522**, 471 (1998).
[25] P. R. C. Kent, M. Jarrell, T. A. Maier, and Th. Pruschke, Phys. Rev. B **72**, 060411(R) (2005).
[26] R. Staudt, M. Dzierzawa, and A. Muramatsu, Eur. Phys. J. B **17**, 411 (2000).
[27] L. De Leo, J. S. Bernier, C. Kollath, A. Georges, and V. W. Scarola, Phys. Rev. A **83**, 023606 (2011).
[28] Trotter errors have been eliminated from the DQMC results and from the Hirsch-Fye QMC [29,30] DMFT data, finite-size effects are negligible for $U/t = 15$ [31].
[29] J. E. Hirsch and R. M. Fye, Phys. Rev. Lett. **56**, 2521 (1986).
[30] N. Blümer, Phys. Rev. B **76**, 205120 (2007).
[31] T. Paiva *et al.* (unpublished).
[32] All scales are set by the root-mean-square energy $\langle \epsilon^2 \rangle_{U=0}^{1/2} = \sqrt{Z}t$ (for coordination number Z) [33].
[33] E. V. Gorelik and N. Blümer, J. Low Temp. Phys. **165**, 195 (2011).
[34] M. Takahashi, J. Phys. C **10**, 1289 (1977).
[35] Zheng Weihong, J. Oitmaa, and C. J. Hamer, Phys. Rev. B **43**, 8321 (1991); A. W. Sandvik, *ibid.* **56**, 11678 (1997).
[36] J. Oitmaa, C. J. Hamer, and Zheng Weihong, Phys. Rev. B **50**, 3877 (1994).
[37] E. V. Gorelik and N. Blümer (unpublished).
[38] J. Sato, B. Aufgebauer, H. Boos, F. Göhmann, A. Klümper, M. Takahashi, and C. Trippe, Phys. Rev. Lett. **106**, 257201 (2011).
[39] Our fit for $d = 3$, $\delta = \infty$ is based on the $T = 0$ order parameter [40], s_N [13], and the critical exponents.
[40] C. M. Soukoulis, S. Datta, and Y. H. Lee, Phys. Rev. B **44**, 446 (1991).
[41] Taking derivatives with respect to the *average* entropy per particle in the inhomogeneous cloud would shift our *central-s* based results slightly toward the T parametrization.
[42] K. G. L. Pedersen, B. M. Andersen, G. M. Bruun, O. F. Syljuåsen, and A. S. Sørensen, Phys. Rev. A **84**, 041603(R) (2011).
[43] M. Pickel, A. B. Schmidt, M. Weinelt, and M. Donath, Phys. Rev. Lett. **104**, 237204 (2010).
[44] This is also to be expected for AF signatures in dynamic properties such as optical conductivity [45].
[45] C. Taranto, G. Sangiovanni, K. Held, M. Capone, A. Georges, and A. Toschi, Phys. Rev. B **85**, 085124 (2012).
[46] U. Schneider, L. Hackermüller, J. P. Ronzheimer, S. Will, S. Braun, T. Best, I. Bloch, E. Demler, S. Mandt, D. Rasch, and A. Rosch, Nat. Phys. **8**, 213 (2012).